

THE EQUIVALENT CIRCUIT OF A MICROSTRIP CROSSOVER

Stilianos Papatheodorou
Roger F. Harrington
Joseph R. Mautz

Department of Electrical and Computer Engineering
Syracuse University
Syracuse, NY 13244-1240

ABSTRACT

The equivalent circuit of a microstrip crossover is found. Integral equations are obtained for the densities of excess charge, and these equations are solved by the method of moments. Introduction of a specified transverse distribution of charge, which satisfies the edge condition, reduces the computing time dramatically while the accuracy remains excellent. Several plots of the excess charge densities are provided along with numerical values of lumped excess capacitances.

This work was supported by the New York State Center for Advanced Technology in Computer Applications and Software Engineering (CASE), Syracuse University, Syracuse, NY 13244, and by the U. S. Army Research Office, Research Triangle Park, NC 27709, under Contract No. DAA03-88-K-0133.

1. INTRODUCTION

A microstrip crossover inside one dielectric layer consists of two nonintersecting striplines perpendicular to each other above a ground plane. Both the striplines have infinite lengths and their widths are $2\alpha_1$ and $2\alpha_2$ for lines 1 and 2 respectively. This structure is referred to as homogeneous since there is no transverse variation of the material properties of the dielectric. The dominant mode is then TEM and the analysis can be carried out using electrostatics (Collin, 1960). The geometry of the problem and the equivalent circuit sought are shown in Figs. 1 and 2 respectively. The microstrip crossover is found in digital circuit boards and in microwave and millimeter wave integrated circuits. In the analysis presented here the proximity of the two striplines produces the so-called excess charges near the discontinuity. These excess charges are related to the line potentials through a pair of coupled integral equations. These equations are then solved via the method of moments with point matching (Harrington, 1968). The results that were obtained were compared to the ones reported by Giri et al (1980) and an excellent agreement was found. We then introduced known charge distributions along the widths of the striplines. This resulted in a dramatic reduction of the computing time, while the accuracy remained excellent.

2. THEORY

Called Q_1 and Q_2 , respectively, the position dependent charges per unit area on lines 1 and 2 can be expressed as

$$Q_1(x,y) = Q_{10}(x) + q_1(x,y) \quad (1)$$

and

$$Q_2(x,y) = Q_{20}(y) + q_2(x,y) \quad (2)$$

If ϕ_1 is the potential of line 1, then Q_{10} is the charge density required to maintain ϕ_1 in the absence of the other line. $Q_{20}(y)$ is defined similarly. As for q_1 and q_2 , they exist in excess of Q_{10} and Q_{20} and they are called excess charge densities. Assuming potentials ϕ_1 and ϕ_2 for lines 1 and 2 we can write

$$\phi_1 = \sum_{j=1}^2 \iint_{S_i} Q_j(x', y') K_{1j} \quad (3)$$

and

$$\phi_2 = \sum_{j=1}^2 \iint_{S_i} Q_j(x', y') K_{2j} \quad (4)$$

Here, S_1 and S_2 are the surfaces of strips 1 and 2 respectively, and K_{ij} is the Green's function kernel given by

$$K_{ij} = \frac{1}{4\pi\epsilon_0} \left[\frac{1}{R_{ij}} - \frac{1}{R_{ij}'} \right] \quad (5)$$

where R_{ij} is the distance between the source point on line j and the field point on line i . Similarly R_{ij}' is the distance between the source point on the image of line j and the field point on line i , $i, j = 1, 2$. We can write (3), (4) in a symbolic form as

$$\phi_1 = \phi(Q_{10}, K_{11}) + \phi(q_1, K_{11}) + \phi(Q_{20}, K_{12}) + \phi(q_2, K_{12}) \quad (6)$$

and

$$\phi_2 = \phi(Q_{20}, K_{22}) + \phi(q_2, K_{22}) + \phi(Q_{10}, K_{21}) + \phi(q_1, K_{21}) \quad (7)$$

From the definitions of Q_{10} and Q_{20} we have

$$\phi_1 = \phi(Q_{10}, K_{11}) \quad (8)$$

$$\phi_2 = \phi(Q_{20}, K_{22}) \quad (9)$$

So that expressions (6)-(7) above become

$$\phi(q_1, K_{11}) + \phi(q_2, K_{12}) = -\phi(Q_{20}, K_{12}) \quad (10)$$

$$\phi(q_1, K_{21}) + \phi(q_2, K_{22}) = -\phi(Q_{10}, K_{21}) \quad (11)$$

The net excess charge of each line is obtained by integrating each excess density over the area of the corresponding strip

$$Q_1^e = \int_{-\infty}^{\infty} dy' \int_{-\alpha_1}^{\alpha_1} dx' q_1(x', y') \quad (12)$$

$$Q_2^e = \int_{-\infty}^{\infty} dx' \int_{-\alpha_2}^{\alpha_2} dy' q_2(x', y') \quad (13)$$

Now we relate these total charges to the line potentials through the coefficients of capacitance and induction (Plonsey and Collin, 1961)

$$Q_1^e = c_{11}\phi_1 + c_{12}\phi_2 \quad (14)$$

$$Q_2^e = c_{21}\phi_1 + c_{22}\phi_2 \quad (15)$$

The lumped excess capacitances are given by

$$C_{11} = c_{11} + c_{12} \quad (16)$$

$$C_{22} = c_{21} + c_{22} \quad (17)$$

$$C_m = -c_{12} \quad (18)$$

In Papatheodorou (April 1988), it is shown that $c_{12} = c_{21}$.

Our objective is to evaluate C_{11} , C_{22} , and C_m . From (8) it is evident that

$$Q_{10} = \phi_1 \hat{Q}_{10} \quad (19)$$

(10) where \hat{Q}_{10} satisfies

$$(11) \quad 1 = \phi(\hat{Q}_{10}, K_{11}) \quad (20)$$

from (9), it is evident that

$$Q_{20} = \phi_2 \hat{Q}_{20} \quad (21)$$

where \hat{Q}_{20} satisfies

$$(12) \quad 1 = \phi(\hat{Q}_{20}, K_{22}) \quad (22)$$

Let now

$$(13) \quad q_1 = \phi_1 \hat{q}_{11} + \phi_2 \hat{q}_{12} \quad (23)$$

$$(24) \quad q_2 = \phi_1 \hat{q}_{21} + \phi_2 \hat{q}_{22}$$

Using (19), (21), (23) and (24) in (10), (11) we find

$$(14) \quad \phi(\hat{q}_{11}, K_{11}) + \phi(\hat{q}_{21}, K_{12}) = 0 \quad (25)$$

$$(15) \quad \phi(\hat{q}_{11}, K_{21}) + \phi(\hat{q}_{21}, K_{22}) = -\phi(\hat{Q}_{10}, K_{21}) \quad (26)$$

and

$$(16) \quad \phi(\hat{q}_{12}, K_{11}) + \phi(\hat{q}_{22}, K_{12}) = -\phi(\hat{Q}_{20}, K_{12}) \quad (27)$$

$$(17) \quad \phi(\hat{q}_{12}, K_{21}) + \phi(\hat{q}_{22}, K_{22}) = 0 \quad (28)$$

On the other hand, use of (23)-(24) in (12)-(13) gives (14)-(15) with

$$(18) \quad c_{1i} = \int_{-\infty}^{\infty} dy' \int_{-\alpha_1}^{\alpha_1} dx' \hat{q}_{1i}(x', y') \quad (29)$$

and

$$(30) \quad c_{2i} = \int_{-\infty}^{\infty} dx' \int_{-\alpha_2}^{\alpha_2} dy' \hat{q}_{2i}(x', y')$$

3. DEVELOPMENT OF MOMENT SOLUTION

To solve (20) for \hat{Q}_{10} , we let

$$\hat{Q}_{10}(x) = \sum_{n=1}^{N_1} a_n P_n(x) \quad (31)$$

where $P_n(x)$ is the pulse function defined by

$$P_n(x) = \begin{cases} 1 & \text{on } \ell_n \\ 0 & \text{elsewhere} \end{cases} \quad (32)$$

Here, ℓ_n is the interval that extends from x_n to x_{n+1} , with

$$x_n = (n-1)\Delta_1 - \alpha_1, \quad n = 1, 2, \dots, N_1+1. \quad (33)$$

where $\Delta_1 = \frac{2\alpha_1}{N_1}$ and N_1 is the number of subsections along the width of

strip 1. In an analogous manner we let

$$\hat{Q}_{20}(y) = \sum_{n=1}^{N_2} b_n P_n(y) \quad (34)$$

where now N_2 is the number of subsections along the width of strip 2. $P_n(y)$ is the pulse function defined by

$$P_n(y) = \begin{cases} 1 & \text{on } \hat{\ell}_n \\ 0 & \text{elsewhere} \end{cases} \quad (35)$$

Here $\hat{\ell}_n$ is the interval that extends from \hat{y}_n to \hat{y}_{n+1} where

$$\hat{y}_n = (n-1)\Delta_2 - \alpha_2, \quad n = 1, 2, \dots, N_2+1 \quad (36)$$

where $\Delta_2 = \frac{2\alpha_2}{N_2}$. Note that throughout this paper circumflexed x_n , and y_n will indicate coordinates for strip 2.

We substitute (31) and (34) into (20) and (22) respectively and enforce (20) at points

$$\{x = x_m^+, \quad m = 1, 2, \dots, N_1\}$$

where

$$x_m^+ = (2m-1) \frac{\Delta_1}{2} - \alpha_1 \quad (37)$$

(31)

and (22) at points

$$\{y = \hat{y}_m^+, \quad m = 1, 2, \dots, N_2\}$$

where

(32)

$$\hat{y}_m^+ = (2m-1) \frac{\Delta_2}{2} - \alpha_2 \quad (38)$$

Then we obtain

(33)

$$\sum_{n=1}^{N_1} f_{mn} a_n = 1, \quad m = 1, 2, \dots, N_1$$

where

(34)

$$f_{mn} = \frac{1}{4\pi\epsilon_0} \int_{x_n}^{x_{n+1}} dx' \int_{-\infty}^{\infty} dy' \left[\frac{1}{\sqrt{(x_m^+ - x')^2 + y'^2}} - \frac{1}{\sqrt{(x_m^+ - x')^2 + y'^2 + 4h_1^2}} \right] \quad (39)$$

and

(35)

$$\sum_{n=1}^{N_2} g_{mn} b_n = 1, \quad m = 1, 2, \dots, N_2$$

where

(36)

$$g_{mn} = \frac{1}{4\pi\epsilon_0} \int_{\hat{y}_n}^{\hat{y}_{n+1}} dy' \int_{-\infty}^{\infty} dx' \left[\frac{1}{\sqrt{(\hat{y}_m^+ - y')^2 + x'^2}} - \frac{1}{\sqrt{(\hat{y}_m^+ - y')^2 + x'^2 + 4h_2^2}} \right] \quad (40)$$

Expressions (39), (40) can now be solved for the unknowns a_n , b_n and then via (31), (34) we evaluate \hat{Q}_{10} , \hat{Q}_{20} respectively.

The excess densities q_1, q_2 vary along the width and length of the corresponding strip. To solve equations (25)-(28) we partition the domain of q_1 and q_2 into rectangular subsections of sides Δ_i , and Δ'_i , $i = 1, 2$. If $2L_i$ is the length of strip i outside of which q_i is assumed to vanish, then along the length of strip i we have N'_i intervals of length

$$\Delta'_i = \frac{2L_i}{N'_i} \quad (41)$$

The n' th interval extends from $y_{n'}$ to $y_{n'+1}$ for strip 1 and from $\hat{x}_{n'}$ to $\hat{x}_{n'+1}$ for strip 2. Note that

$$y_{n'} = (n'-1)\Delta'_1 - L_1 \quad (42)$$

and

$$\hat{x}_{n'} = (n'-1)\Delta'_2 - L_2 \quad (43)$$

As it is suggested by Mautz and Harrington (1984) a total length of about $2h_2$ will give satisfactory results.

Next let

$$\hat{q}_{1i} = \sum_{n=1}^{N_1} \sum_{n'=1}^{N'_1} \hat{q}_{1i,nn'} P_{nn'} \quad (44)$$

$$\hat{q}_{2i} = \sum_{n=1}^{N_2} \sum_{n'=1}^{N'_2} \hat{q}_{2i,nn'} P_{nn'} \quad (45)$$

$$\text{Here } P_{nn'} = \begin{cases} 1 & \text{on } \Delta s_{nn'} \\ 0 & \text{elsewhere} \end{cases} \quad i = 1, 2$$

and $\Delta s_{nn'}$ is the nn' th rectangular subsection with domain

$$(x_n \leq x < x_{n+1}, y_{n'} \leq y < y_{n'+1}) \quad \text{for strip 1}$$

and domain

$$(\hat{x}_{n'} \leq x < \hat{x}_{n'+1}, \hat{y}_n \leq y < \hat{y}_{n+1}) \quad \text{for strip 2.}$$

We then substitute (44), (45), (31), and (34) into (25)-(28) and enforce (25), (27) at points

$$\{(x,y) = (x_m^+, y_m^+), m = 1,2,\dots,N_1 \text{ and } m' = 1,2,\dots,N_1'\}$$

where now y_m^+ is the midpoint of the subsection that extends from y_m to $y_{m'+1}$ and is given by

$$y_m^+ = (2m'-1) \frac{\Delta_1'}{2} - L_1 \quad (46)$$

Similarly we enforce (26), (28) at points

$$\{(x,y) = (\hat{x}_m^+, \hat{y}_m^+), m = 1,2,\dots,N_2 \text{ and } m' = 1,2,\dots,N_2'\}$$

where \hat{x}_m^+ is now the midpoint of the subsection that extends from \hat{x}_m to $\hat{x}_{m'+1}$ and given by

$$\hat{x}_m^+ = (2m'-1) \frac{\Delta_2'}{2} - L_2 \quad (47)$$

\hat{y}_m^+ is the midpoint along the width given by (38), which is repeated for convenience

$$\hat{y}_m^+ = (2m-1) \frac{\Delta_2}{2} - \alpha_2 \quad (48)$$

We thus obtain the systems

$$[k] \begin{bmatrix} \vec{q}_{11} \\ \vec{q}_{21} \end{bmatrix} = \begin{bmatrix} 0 \\ -[l] \vec{a} \end{bmatrix} \quad (49)$$

$$[k] \begin{bmatrix} \vec{q}_{12} \\ \vec{q}_{22} \end{bmatrix} = \begin{bmatrix} -[g] \vec{b} \\ 0 \end{bmatrix} \quad (50)$$

Here \vec{a} , \vec{b} are the vectors formed by the coefficients a_n , b_n of (31), (34)

respectively. The elements of the system matrix k and the forcing matrices ℓ and g are given in Appendix A.

4. MODIFIED SOLUTION

The systems of equations given by (49) and (50) contain a large number of unknowns. If we could eliminate the unknowns that describe the variation of the charge densities along the width of each stripline we would reduce to size of the system matrix substantially. To this end we introduce an edge behavior proposed by Butler and Wilton (1980). Then (31) and (34) are replaced by

$$\hat{Q}_{10}(x) \cong \frac{G_1}{\sqrt{\alpha_1^2 - x^2}} \quad (51)$$

and

$$\hat{Q}_{20}(y) \cong \frac{G_2}{\sqrt{\alpha_2^2 - y^2}} \quad (52)$$

respectively. Introducing (51), (52) into (20), (22) we obtain after a straightforward integration

$$4\pi\epsilon_0 = G_1 \int_{-\alpha_1}^{\alpha_1} \frac{dx'}{\sqrt{\alpha_1^2 - x'^2}} \ln \left[\frac{(x-x')^2 + 4h_1^2}{(x-x')^2} \right] \quad (53)$$

and

$$4\pi\epsilon_0 = G_2 \int_{-\alpha_2}^{\alpha_2} \frac{dy'}{\sqrt{\alpha_2^2 - y'^2}} \ln \left[\frac{(y-y')^2 + 4h_2^2}{(y-y')^2} \right] \quad (54)$$

G_1, G_2 are constants that can be computed from relations (53), (54) above. This is shown in Appendix B.

rices

In a similar manner expressions (44) and (45) are replaced by

$$\hat{q}_{1i} = \frac{1}{\sqrt{\alpha_1^2 - x^2}} \sum_{n'=1}^{N'_1} \hat{q}_{1i,n'} P_{n'}(y) \quad (55)$$

and

$$\hat{q}_{2i} = \frac{1}{\sqrt{\alpha_2^2 - y^2}} \sum_{n'=1}^{N'_2} \hat{q}_{2i,n'} P_{n'}(x), \quad i = 1, 2 \quad (56)$$

he

respectively. Then we substitute (55), (56), (51), and (52) into (25)-(28) and enforce (25), (27) at points

$$\{(x, y) = (0, y_m^+), \quad m' = 1, 2, \dots, N'_1\} \quad (57)$$

(51)

and (26), (28) at points

$$\{(x, y) = (\hat{x}_m^+, 0), \quad m' = 1, 2, \dots, N'_2\} \quad (58)$$

(52)

Note that y_m^+ , \hat{x}_m^+ are still given by (46), (47) respectively. Thus the system of equations that is obtained now is of the form

$$[k'] \begin{bmatrix} \vec{q}_{11} \\ \vec{q}_{21} \end{bmatrix} = \begin{bmatrix} 0 \\ -G_1 \vec{\ell} \end{bmatrix} \quad (59)$$

(53)

and

$$[k'] \begin{bmatrix} \vec{q}_{12} \\ \vec{q}_{22} \end{bmatrix} = \begin{bmatrix} -G_2 \vec{g} \\ 0 \end{bmatrix} \quad (60)$$

(54)

The new system matrix has now considerably fewer elements which along with the forcing vectors $\vec{\ell}$ and \vec{g} are described in Appendix B.

a.

5. NUMERICAL RESULTS AND DISCUSSION

Giri et al. (1980) presented a solution for two skewed wire lines above a ground plane. For the sake of comparison we have solved the same problem when the two wires were perpendicular to each other, that is, the wire crossover (Papatheodorou et al., April 1988). When we compare the excess density plots the agreement is excellent. We then solved the strip crossover using the theory presented in Section 3 of this paper. The widths of the strip were chosen according to Butler (1982) who shows that a narrow strip line is equivalent to a wire line when the strip has width equal to four times the wire radius (equivalent radius). Therefore for a wire crossover with wire radius equal to $10^{-2}h_1$ the strips had widths equal to $4 \times 10^{-2}h_1$. The height ratio $\frac{h_2}{h_1}$ was taken equal to 1.5 and each subsection across the length of both the wire and the strip was taken equal to $5 \times 10^{-2}h_1$. We chose $L_1 = L_2 = 5h_1$. Figures 3-6 show the plots of the excess densities versus the normalized distance from the center of symmetry. For the wire lines we have plotted

$$\frac{\hat{q}_{1i}^w}{C'_i} \quad \text{and} \quad \frac{\hat{q}_{2i}^w}{C'_i}, \quad i = 1, 2,$$

where C'_i is the capacitance per unit length of the i th isolated line. On the other hand, for the strip lines we have plotted $\frac{\tilde{q}_{1i}}{C'_i}$ where

$$\tilde{q}_{1i}(y) = \int_{-\alpha_1}^{\alpha_1} \hat{q}_{1i}(x, y) dx \quad (61)$$

and $\frac{\tilde{q}_{2i}}{C'_i}$ where

$$\tilde{q}_{2i}(x) = \int_{-\alpha_2}^{\alpha_2} \hat{q}_{2i}(x, y) dy, \quad i = 1, 2. \quad (62)$$

In Figs. 3-6 the strips were divided along the widths into 6 subsections. The agreement between the wire and the strip solution is very good and the lumped normalized excess capacitances found are

$$\frac{C_m}{h_1 C_2'} = 1.013, \quad \frac{C_{11}}{h_1 C_1'} = -0.853, \quad \text{and} \quad \frac{C_{22}}{h_1 C_2'} = -0.792 \quad \text{for the wire}$$

and

$$\frac{C_m}{h_1 C_2'} = 0.991, \quad \frac{C_{11}}{h_1 C_1'} = -0.836, \quad \text{and} \quad \frac{C_{22}}{h_1 C_2'} = -0.777$$

for the strip crossover. The strip results are even closer to those for the wire when more subsections along the width of the strips are used. For example when 12 instead of 6 subsections are used the capacitances are found to be

$$\frac{C_m}{h_1 C_2'} = 1.002, \quad \frac{C_{11}}{h_1 C_1'} = -0.844, \quad \text{and} \quad \frac{C_{22}}{h_1 C_2'} = -0.785$$

However, the price that we paid was an increase in the CPU time from one hour and fourteen minutes to more than five hours on a VAX 8810.

When the solution of Section 4 was used the CPU time reduces down to a minute and forty eight seconds, while the accuracy remains excellent. The strip parameters were kept the same and Fig. 7 shows the charge densities for this solution. The normalized capacitances in this case were found to be

$$\frac{C_m}{h_1 C_2'} = 1.014, \quad \frac{C_{11}}{h_1 C_1'} = -0.853, \quad \text{and} \quad \frac{C_{22}}{h_1 C_2'} = -0.792,$$

which are almost identical to the capacitances of the wire crossover. It should be emphasized however, that this excellent agreement happens only for narrow strips.

APPENDIX A

The system matrix of relations (49) and (50) is of the form

$$[k] = \begin{bmatrix} [k^{11}] & [k^{12}] \\ [k^{21}] & [k^{22}] \end{bmatrix} \quad (A-1)$$

The submatrices k^{11} , k^{12} , k^{21} and k^{22} have $mm'nn'$ th elements given by

$$k_{mm'nn'}^{11} = \int_{x_n}^{x_{n+1}} dx' \int_{y_{n'}}^{y_{n'+1}} dy' \left[\frac{1}{\sqrt{(x_m^+ - x')^2 + (y_{m'}^+ - y')^2}} - \frac{1}{\sqrt{(x_m^+ - x')^2 + (y_{m'}^+ - y')^2}} \right] \quad (A-2)$$

$$k_{mm'nn'}^{12} = \int_{\hat{y}_n}^{\hat{y}_{n+1}} dy' \int_{\hat{x}_n}^{\hat{x}_{n+1}} dx' \left[\frac{1}{\sqrt{(x_m^+ - x')^2 + (y_{m'}^+ - y')^2 + (h_2 - h_1)^2}} - \frac{1}{\sqrt{(x_m^+ - x')^2 + (y_{m'}^+ - y')^2 + (h_2 + h_1)^2}} \right] \quad (A-3)$$

$$k_{mm'nn'}^{21} = \int_{x_n}^{x_{n+1}} dx' \int_{y_{n'}}^{y_{n'+1}} dy' \left[\frac{1}{\sqrt{(\hat{x}_m^+ - x')^2 + (\hat{y}_{m'}^+ - y')^2 + (h_2 - h_1)^2}} - \frac{1}{\sqrt{(\hat{x}_m^+ - x')^2 + (\hat{y}_{m'}^+ - y')^2 + (h_2 + h_1)^2}} \right] \quad (A-4)$$

and

$$k_{mm'nn'}^{22} = \int_{\hat{y}_n}^{\hat{y}_{n+1}} dy' \int_{\hat{x}_n}^{\hat{x}_{n'+1}} dx' \left[\frac{1}{\sqrt{(\hat{x}_m^+ - x')^2 + (\hat{y}_m^+ - y')^2}} - \frac{1}{\sqrt{(\hat{x}_m^+ - x')^2 + (\hat{y}_m^+ - y')^2 + 4h_2^2}} \right] \quad (A-5)$$

respectively.

The evaluation of the above elements is straightforward but tedious and is given in Appendix A of Papatheodorou, Harrington, and Mautz (April, 1988).

The m'nth element of the forcing matrix ℓ is given after a straightforward integration by

$$\ell_{m'n} = \int_{x_n}^{x_{n+1}} dx' \ell_n \left[\frac{(\hat{x}_m^+ - x')^2 + (h_2 + h_1)^2}{(\hat{x}_m^+ - x')^2 + (h_2 - h_1)^2} \right] \quad (A-6)$$

Using Dwight (1961) this becomes

$$\ell_{m'n} = \left[x \ell_n \left(\frac{x^2 + (h_2 + h_1)^2}{x^2 + (h_2 - h_1)^2} \right) + 2(h_2 + h_1) \tan^{-1} \left(\frac{x}{h_2 + h_1} \right) - 2(h_2 - h_1) \tan^{-1} \left(\frac{x}{h_2 - h_1} \right) \right] \Bigg|_{x=x_n - \hat{x}_m^+}^{x_{n+1} - \hat{x}_m^+} \quad (A-7)$$

The m'nth element of forcing matrix g is given by a similar expression.

APPENDIX B

i) Evaluation of constant G_1, G_2

The integrals that appear in relations (53) and (54) are solved numerically using an efficient algorithm, the Gauss-Chebyshev quadrature (Carnahan, Luther, and Wilkes, 1969). However, the denominator in the argument of \ln can become singular and needs special attention. To handle this we enforce (53) at $x=0$ and after a simple variable transformation we write

$$4\pi\epsilon_0 = G_1 \int_{-1}^1 \frac{dx'}{\sqrt{1-x'^2}} \ln [(\alpha_1 x')^2 + 4h_1^2] - G_1 \int_{-1}^1 \frac{dx'}{\sqrt{1-x'^2}} \ln (\alpha_1 x')^2 \quad (B-1)$$

Using Dwight (1961) the second integral is simply equal to $2\pi \ln (\frac{\alpha_1}{2})$. Applying the Gauss-Chebyshev algorithm for the first integral we find that G_1 is given by

$$G_1 = \frac{4\epsilon_0}{\frac{1}{n+1} \sum_{i=0}^n \ln [(\alpha_1 x_i)^2 + 4h_1^2] - 2 \ln \frac{\alpha_1}{2}} \quad (B-2)$$

Here n is the number of points used in the quadrature formula and x_i is given by

$$x_i = \cos \left[\frac{(2i+1)\pi}{(2n+2)} \right], \quad i = 0, 1, \dots, n \quad (B-3)$$

G_2 is given by (B-2) if we replace α_1 and h_1 with α_2 and h_2 respectively.

ii) The system matrix k

Again the system matrix in (59) and (60) is of the form given in

(A-1). However, the submatrix elements are simpler. So we have

$$k_{m'n'}^{11} = \int_{-\alpha_1}^{\alpha_1} \frac{dx'}{\sqrt{\alpha_1^2 - x'^2}} \int_{y_n}^{y_{n'+1}} dy' \left[\frac{1}{\sqrt{x'^2 + (y_m^+ - y')^2}} - \frac{1}{\sqrt{x'^2 + (y_m^+ - y')^2 + 4h_1^2}} \right] \quad (\text{B-4})$$

$$k_{m'n'}^{12} = \int_{-\alpha_2}^{\alpha_2} \frac{dy'}{\sqrt{\alpha_2^2 - y'^2}} \int_{\hat{x}_n}^{\hat{x}_{n'+1}} dx' \left[\frac{1}{\sqrt{x'^2 + (y_m^+ - y')^2 + (h_2 - h_1)^2}} - \frac{1}{\sqrt{x'^2 + (y_m^+ - y')^2 + (h_2 + h_1)^2}} \right] \quad (\text{B-5})$$

$$k_{m'n'}^{21} = \int_{-\alpha_1}^{\alpha_1} \frac{dx'}{\sqrt{\alpha_1^2 - x'^2}} \int_{y_n}^{y_{n'+1}} dy' \left[\frac{1}{\sqrt{(\hat{x}_m^+ - x')^2 + y'^2 + (h_2 - h_1)^2}} - \frac{1}{\sqrt{(\hat{x}_m^+ - x')^2 + y'^2 + (h_2 + h_1)^2}} \right] \quad (\text{B-6})$$

$$k_{m'n'}^{22} = \int_{-\alpha_2}^{\alpha_2} \frac{dy'}{\sqrt{\alpha_2^2 - y'^2}} \int_{\hat{x}_n}^{\hat{x}_{n'+1}} dx' \left[\frac{1}{\sqrt{(\hat{x}_m^+ - x')^2 + y'^2}} - \frac{1}{\sqrt{(\hat{x}_m^+ - x')^2 + y'^2 + 4h_2^2}} \right] \quad (\text{B-7})$$

After a straightforward integration expressions (8-5), (B-6) can be evaluated numerically using the same algorithm as in (i). However, in expressions (B-4), (B-7) we should be more careful due to occurring singularities. The explicit evaluation of these relations is shown in Appendix B of Papatheodorou, Harrington, and Mautz (July, 1988).

iii) The forcing vectors $\vec{\ell}$ and \vec{g}

The m'th element of the forcing vector $\vec{\ell}$ is of the form

$$\ell_{m'} = \int_{-\alpha_1}^{\alpha_1} \frac{dx'}{\sqrt{\alpha_1^2 - x'^2}} \ln \left[\frac{(\hat{x}_m^+ - x')^2 + (h_2 + h_1)^2}{(\hat{x}_m^+ - x')^2 + (h_2 - h_1)^2} \right] \quad (\text{B-8})$$

After a simple variable transformation, $\ell_{m'}$ can be easily evaluated using the Gauss-Chebyshev quadrature, which gives

$$\ell_{m'} = \frac{\pi}{n+1} \sum_{i=0}^n \ln \left[\frac{(\hat{x}_m^+ - \alpha_1 x_i)^2 + (h_2 + h_1)^2}{(\hat{x}_m^+ - \alpha_1 x_i)^2 + (h_2 - h_1)^2} \right] \quad (\text{B-9})$$

As for $g_{m'}$, it is obtained from $\ell_{m'}$ by replacing α_1 and \hat{x}_m^+ with α_2 and y_m^+ , respectively. Again n is the number of points used in the quadrature formula and x_i is given by (B-3).

Dwight, H. B., 1961. Tables of Integrals and Other Mathematical Data, Macmillan, New York.

Papatheodorou, S., Harrington, R. F. and Mautz, J. R., July 1988.

"A Quasi-Static Analysis of a Microstrip Crossover Using a Prescribed Transverse Charge Distribution," Technical Report TR-88-4, Department of Electrical and Computer Engineering, Syracuse University, Syracuse, New York 13244-1240.

Butler, C. M., July 1982. "The Equivalent Radius of a Narrow Conducting Strip," IEEE Trans. Antennas Propagat., vol. AP-30, pp. 755-758.

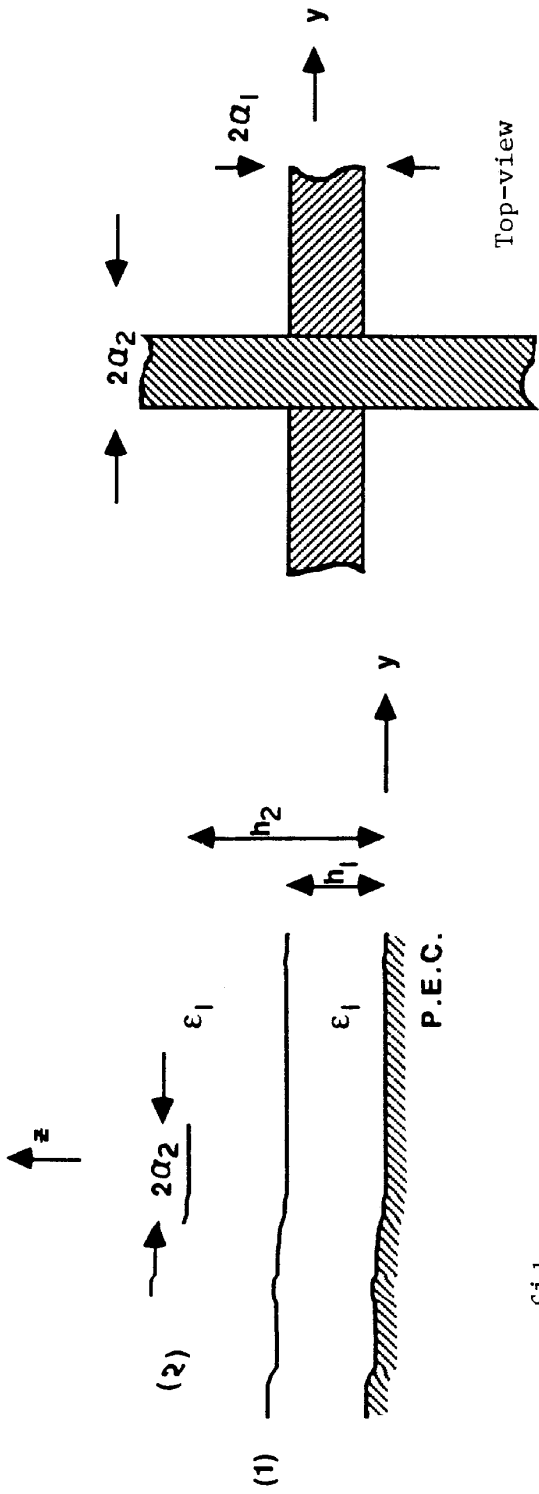


Fig. 1. Geometry of the microstrip crossover.

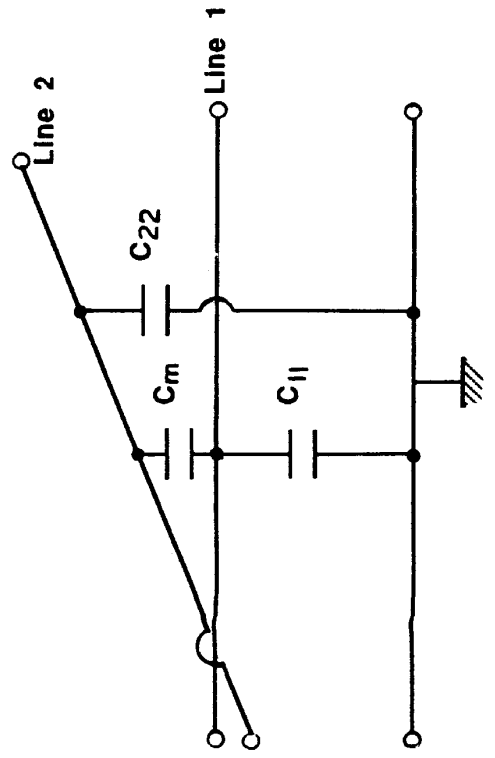


Fig. 2. Equivalent circuit of the microstrip crossover.

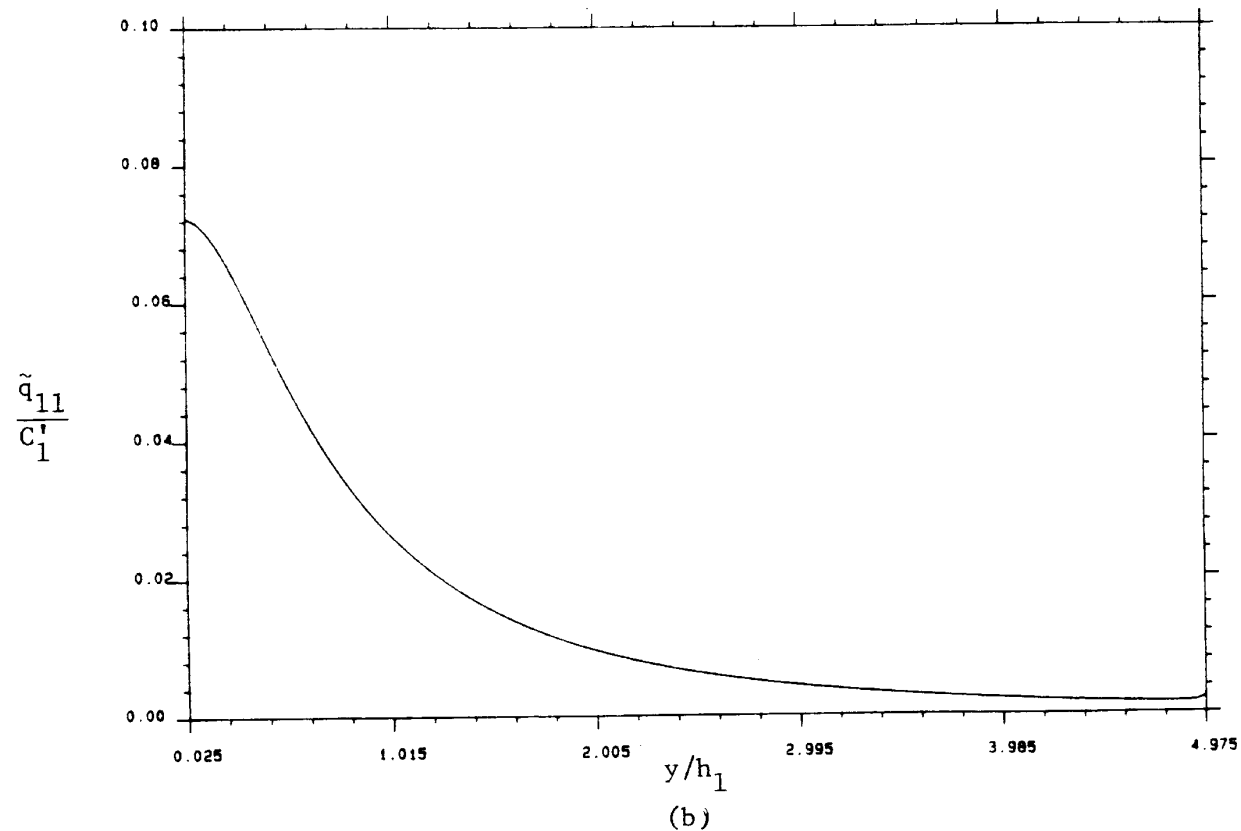
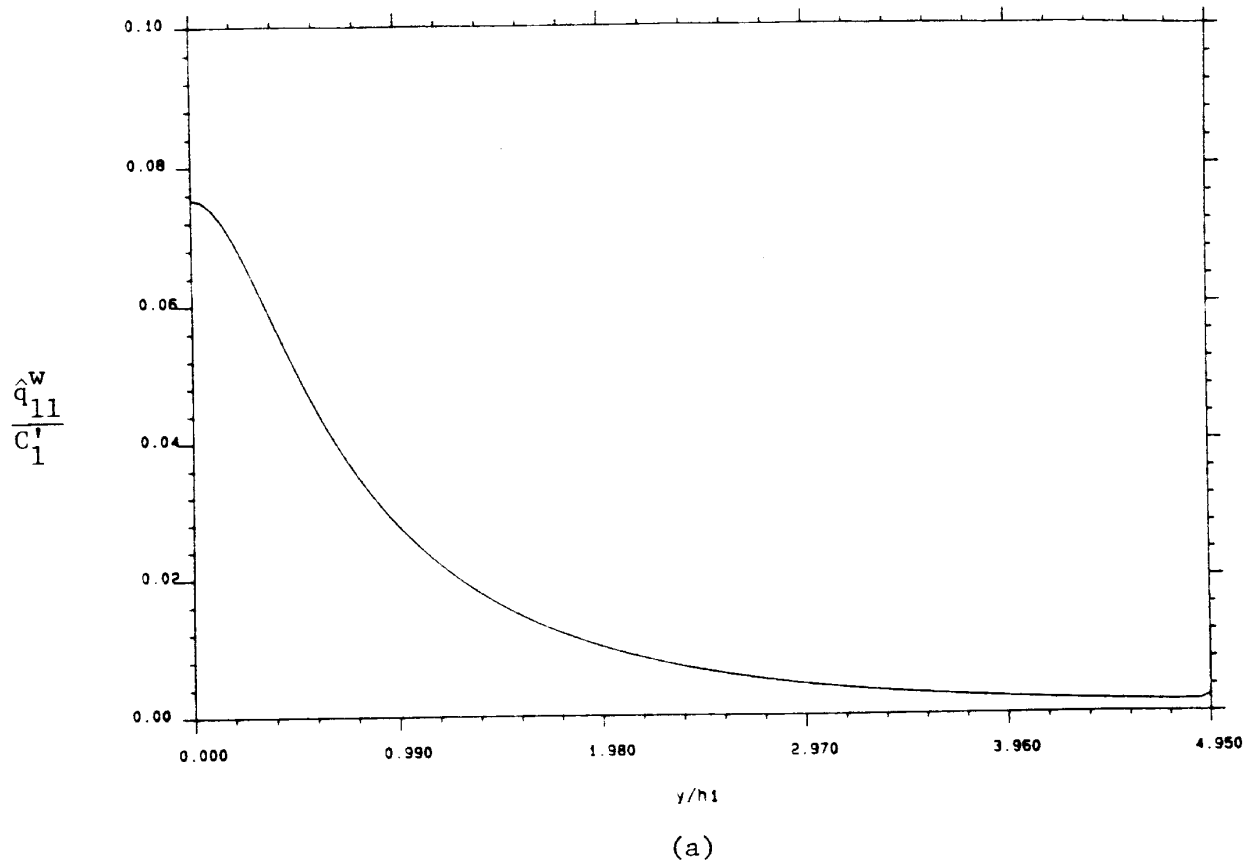


Fig. 3. Normalized excess charge densities along (a) two lines and (b) two strip lines. Here $h_2/h_1 = 1.5$, wire radius = $0.01 h_1$, strip width = $0.04 h_1$.

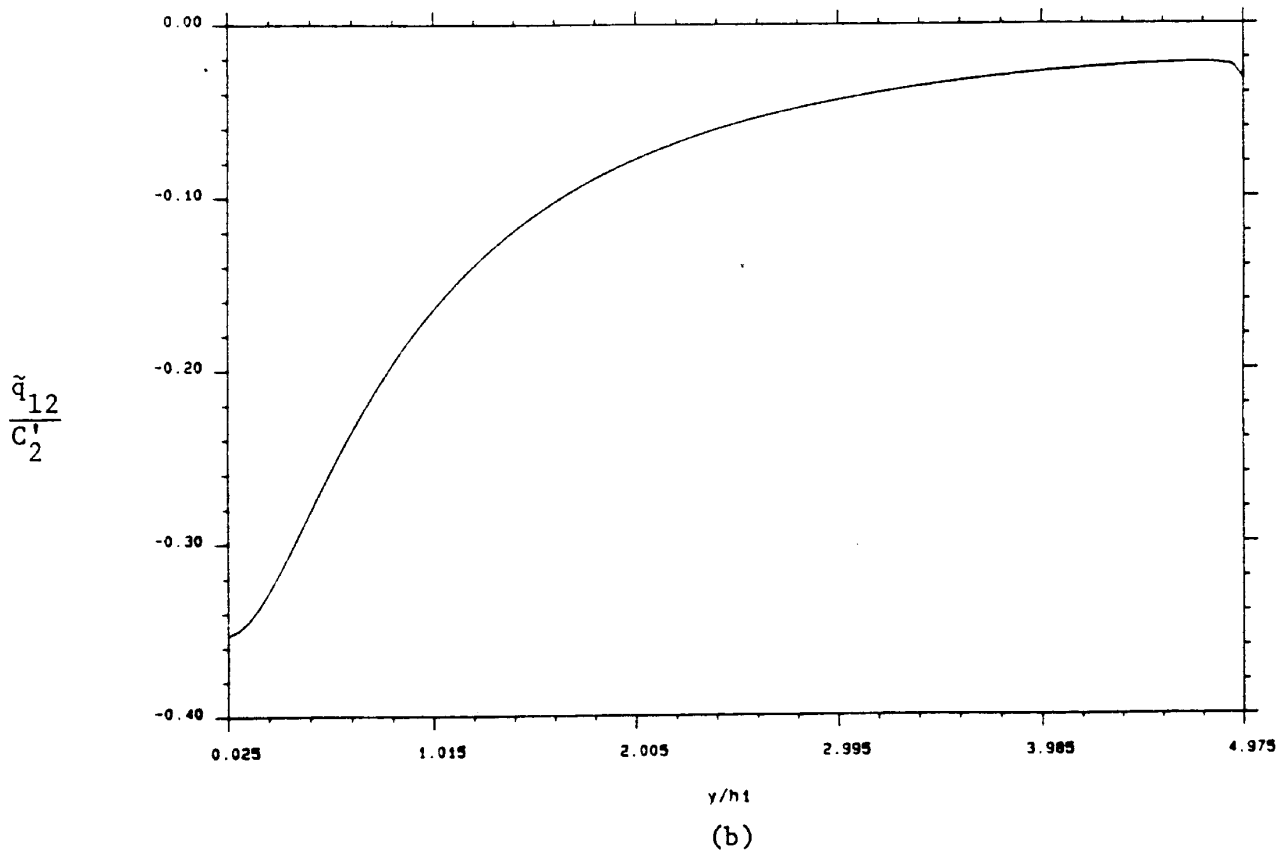
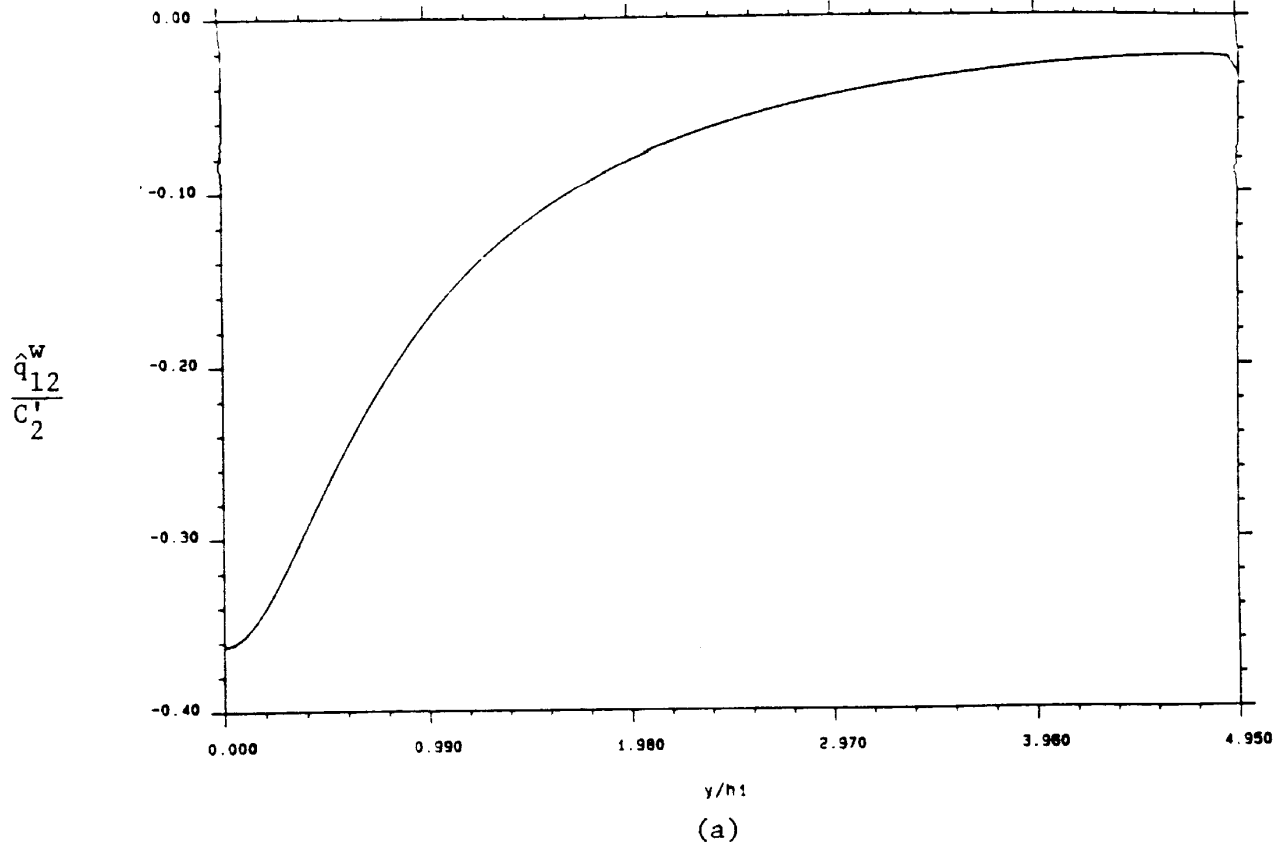
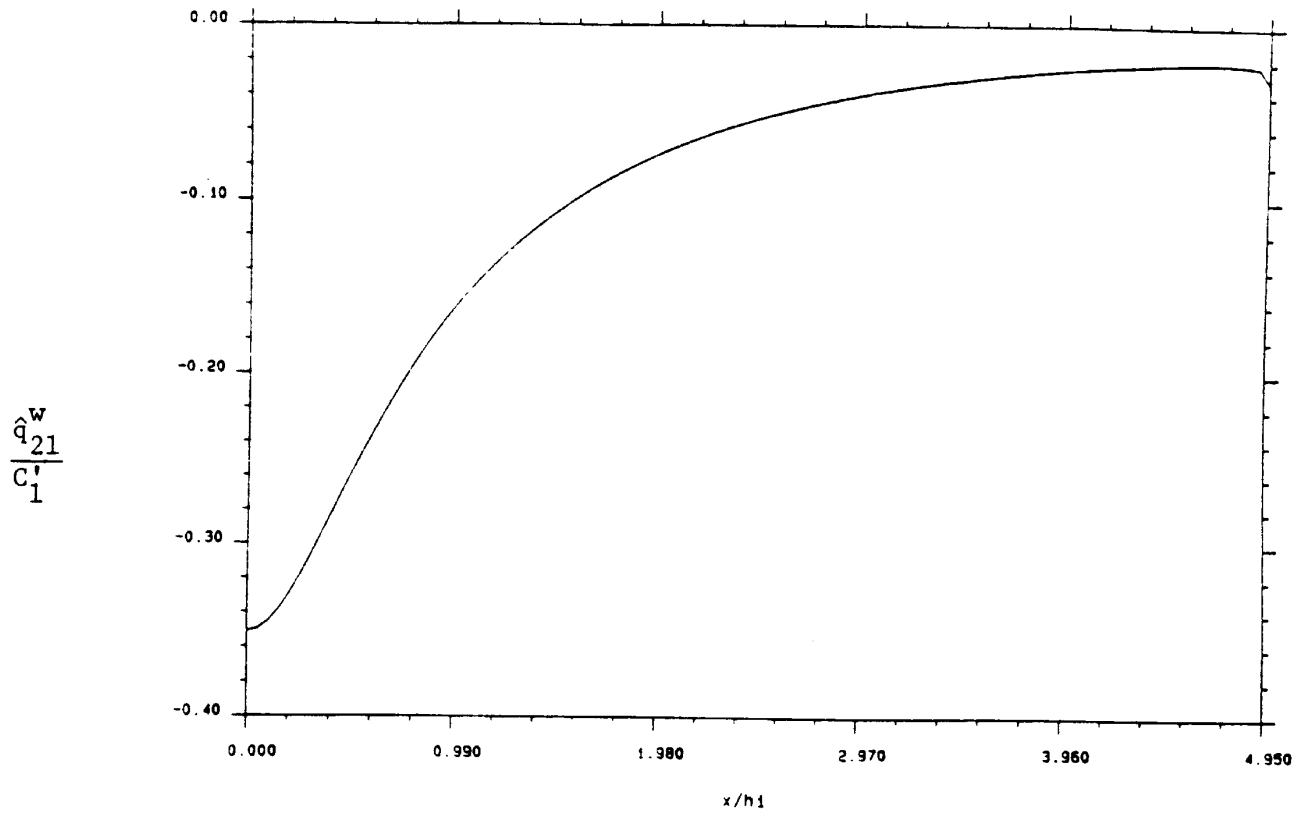
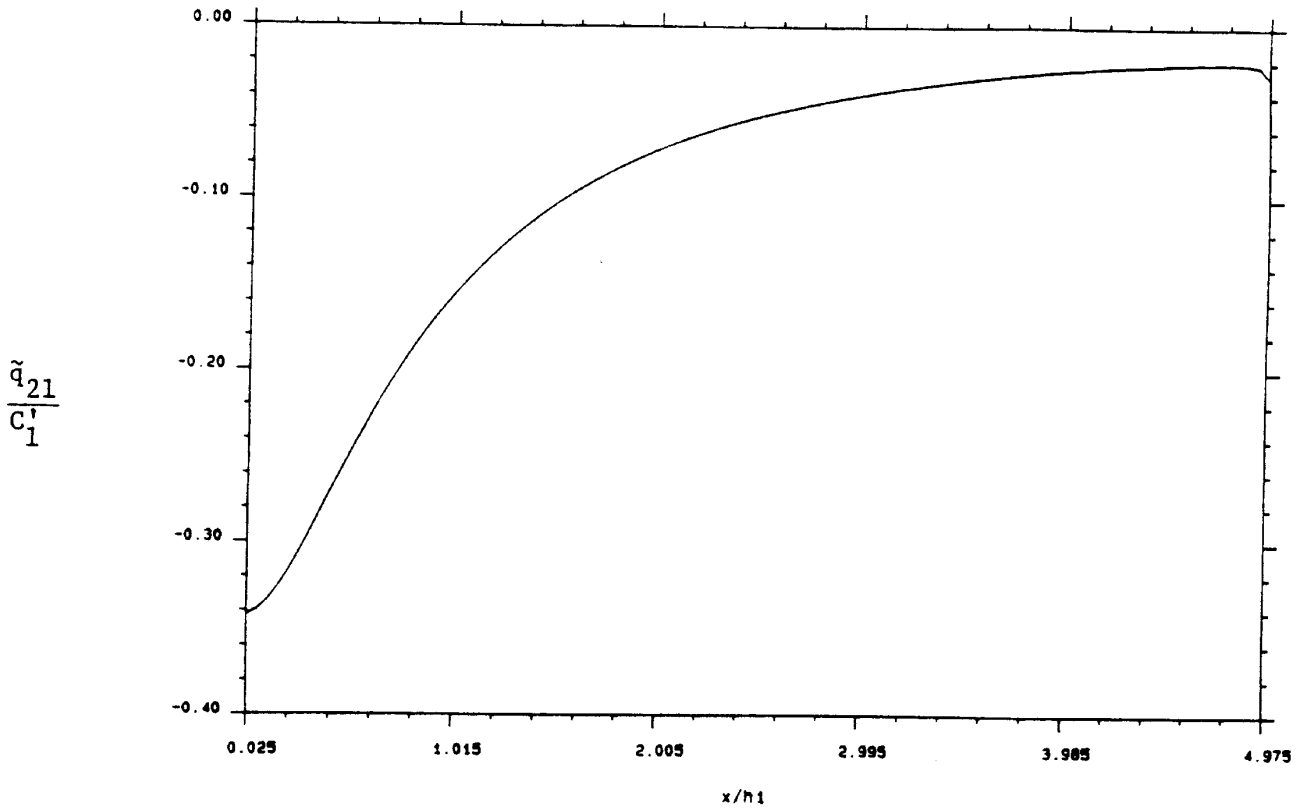


Fig. 4. Normalized excess charge densities along (a) two lines and (b) two strip lines. Here $h_2/h_1 = 1.5$, wire radius = $0.01 h_1$, strip width = $0.04 h_1$.



(a)



(b)

Fig. 5. Normalized excess charge densities along (a) two lines and (b) two strip lines. Here $h_2/h_1 = 1.5$, wire radius = $0.01 h_1$, strip width = $0.04 h_1$.

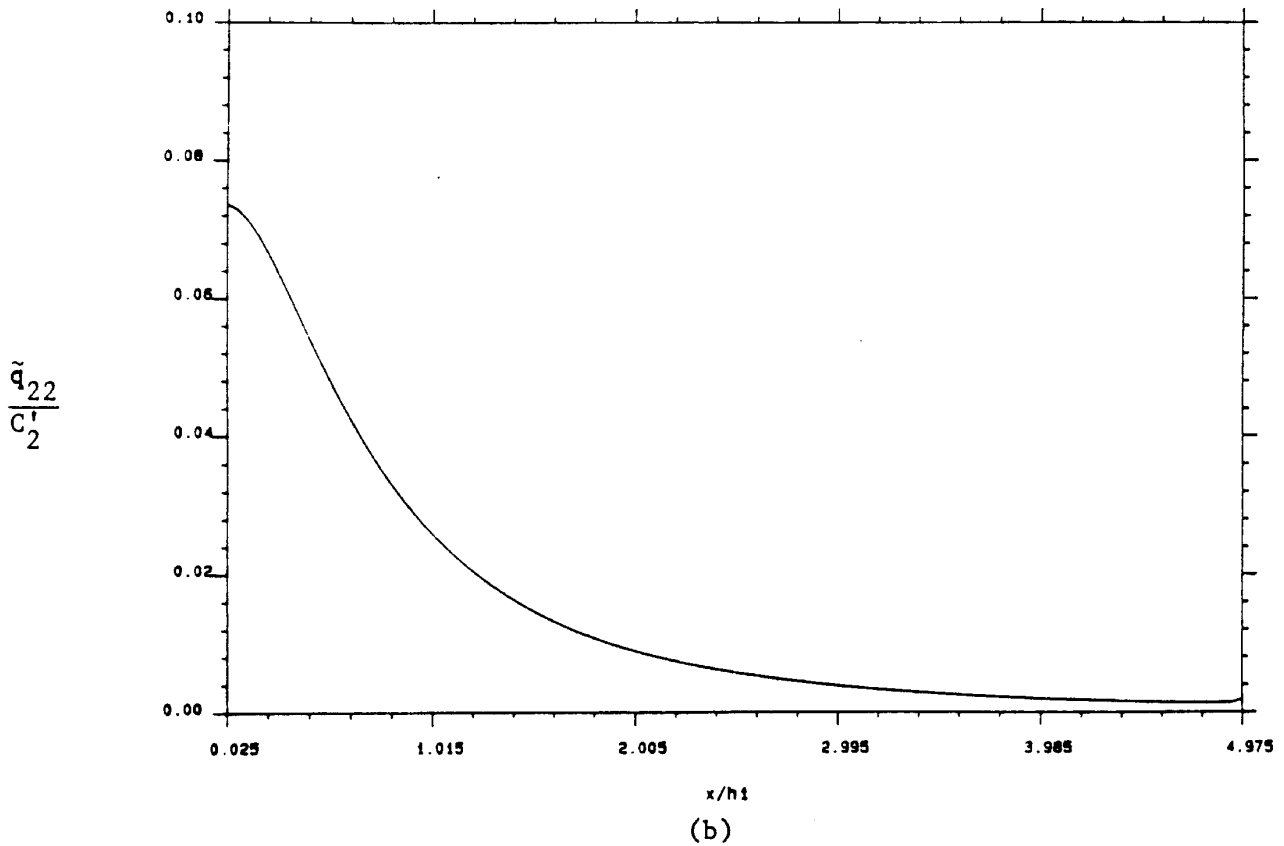
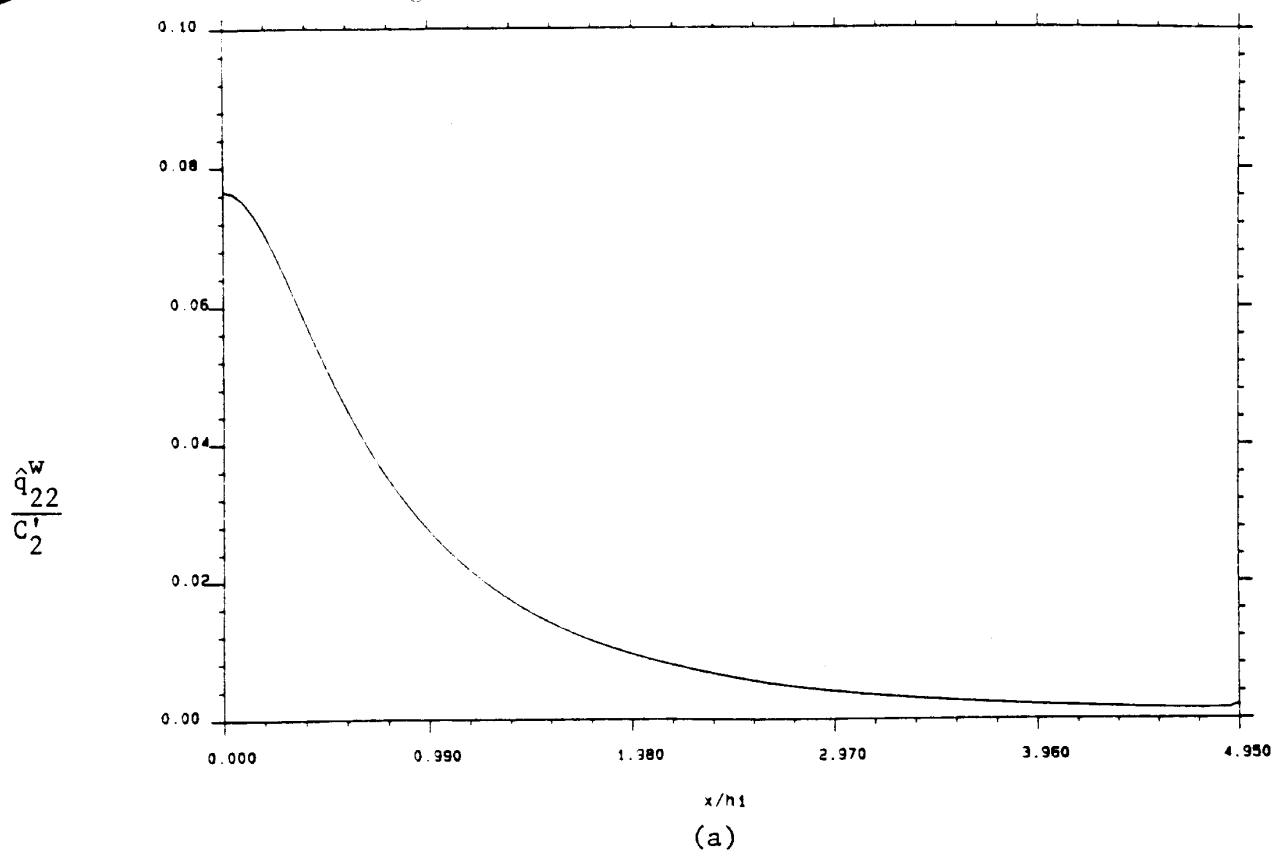


Fig. 6. Normalized excess charge densities along (a) two lines and (b) two strip lines. Here $h_2/h_1 = 1.5$, wire radius = $0.01 h_1$, strip width = $0.04 h_1$.

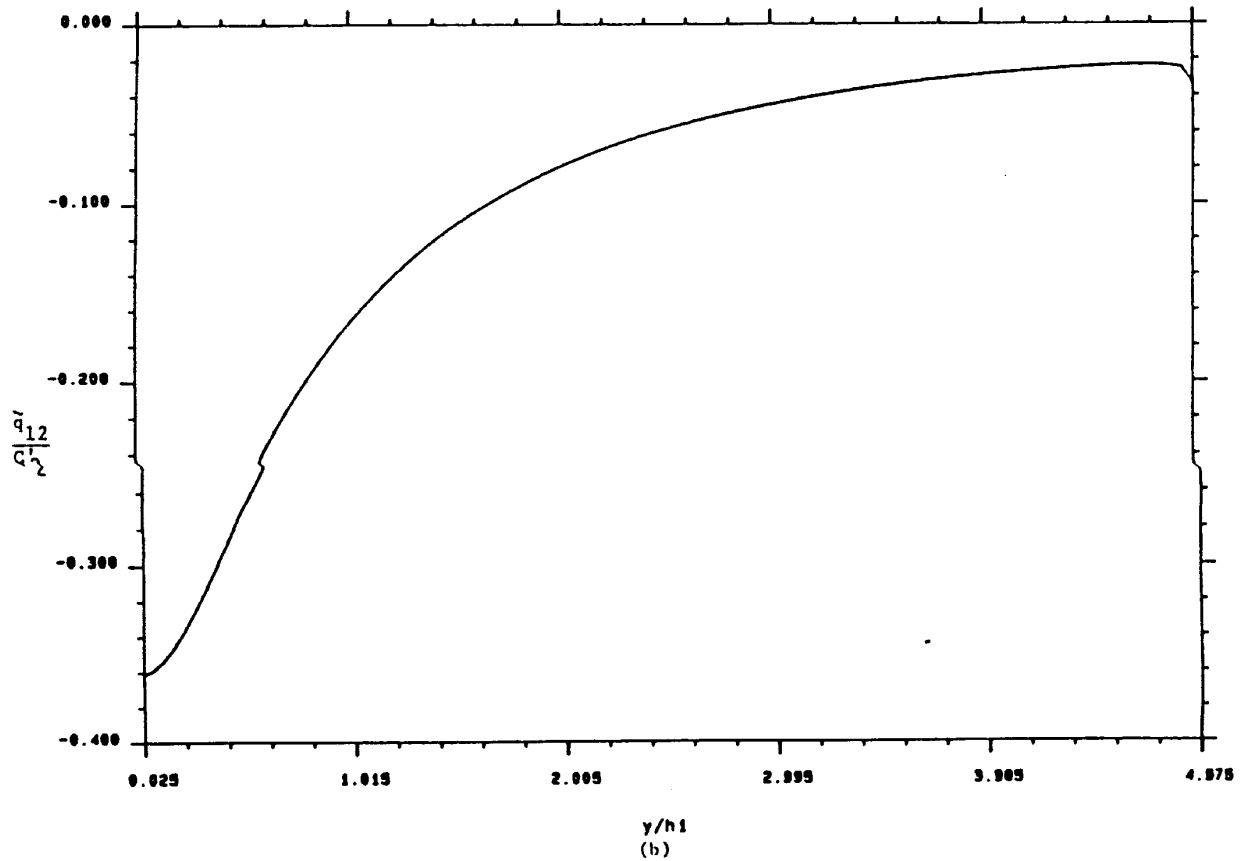
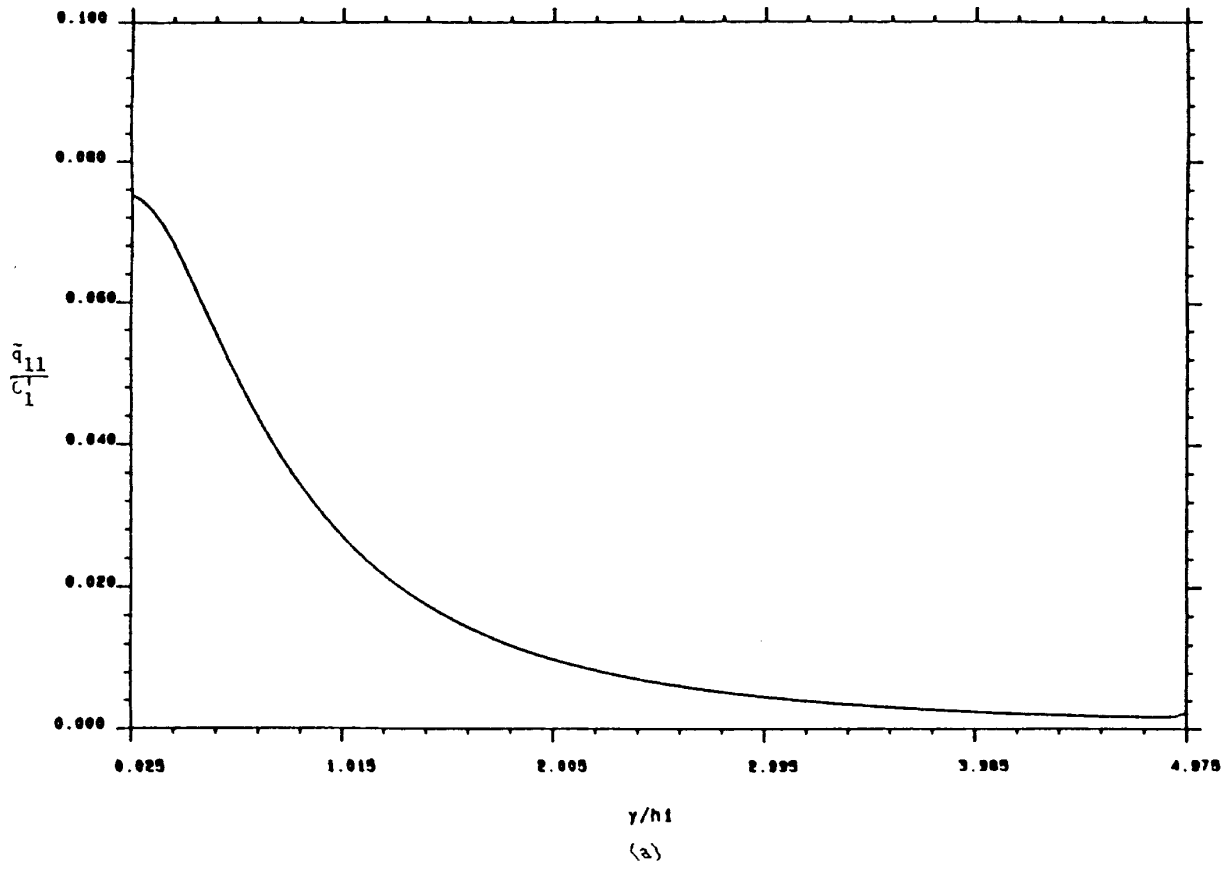


Fig. 7. (a)-(d). Normalized excess charge densities when the edge condition of section 4 was used. The strip parameters are the same as in Figs. 3-6.

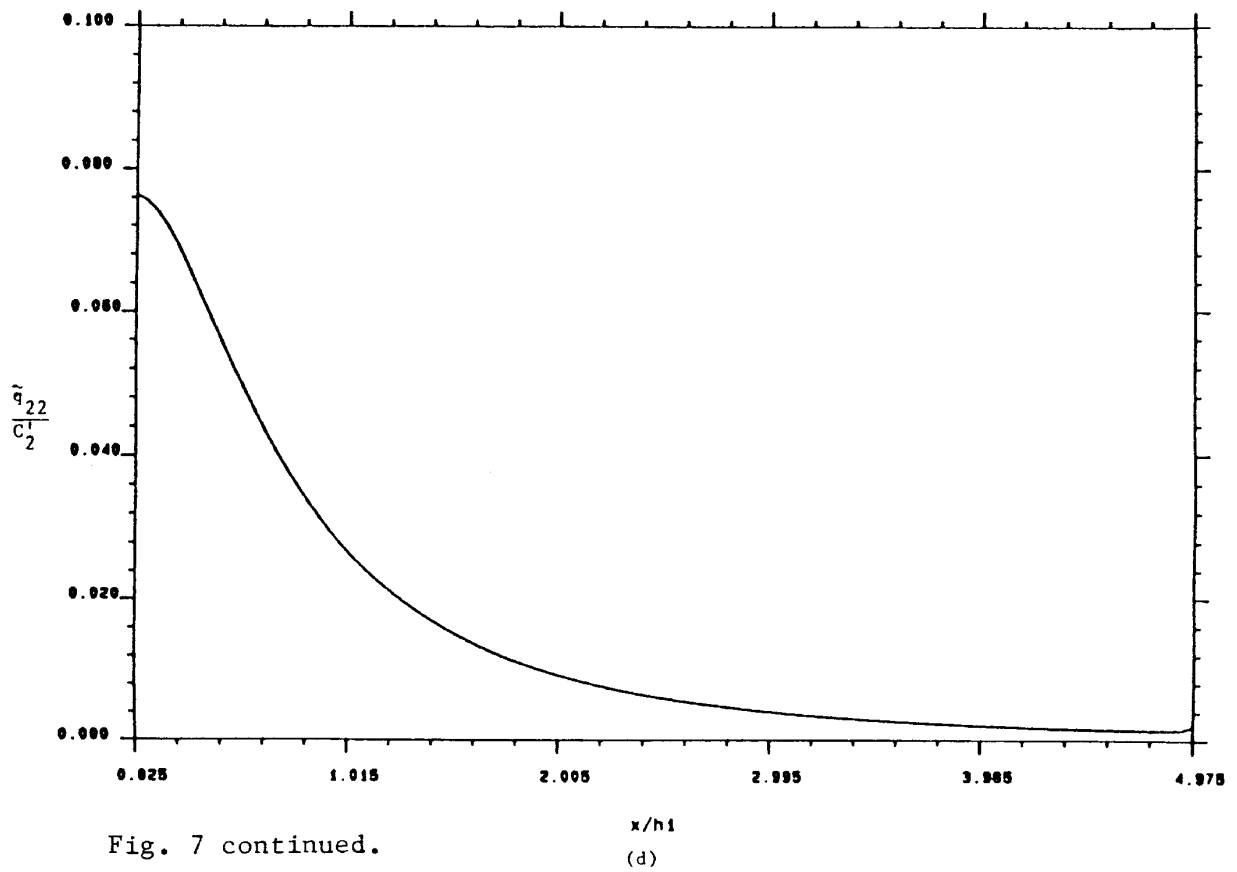
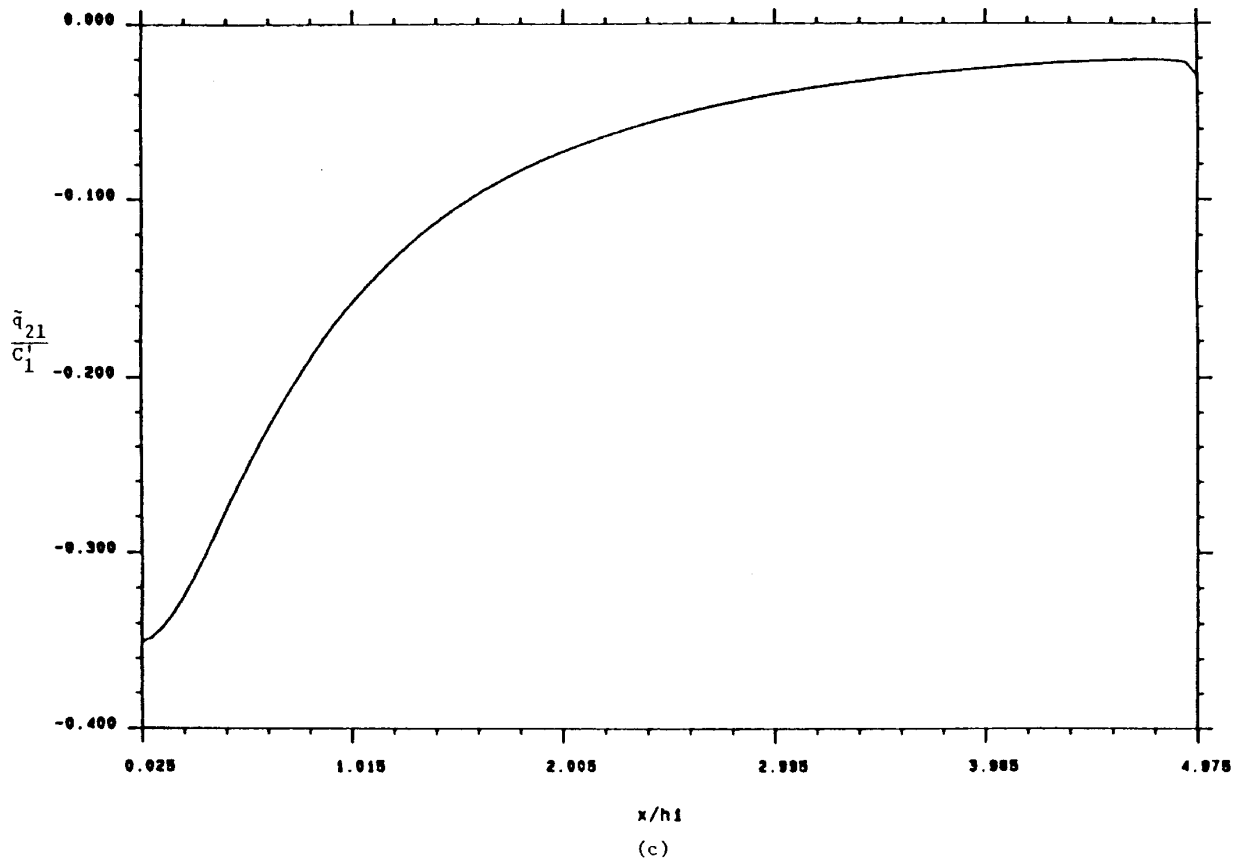


Fig. 7 continued.